Engineering Solid Mechanics 4 (2016) 97-108

Contents lists available at GrowingScience

Engineering Solid Mechanics

homepage: www.GrowingScience.com/esm

Exact solution for whirling analysis of axial-loaded Timoshenko rotor using basic functions

K. Torabi* and H. Afshari

Faculty of mechanical engineering, University of Kashan, Kashan, Iran

ARTICLE INFO

Article history:
Received 6 April, 2015
Accepted 24 November 2015
Available online
25 November 2015

Keywords:
Basic functions
Whirling analysis
Timoshenko rotor
Axial load

ABSTRACT

In this paper, an analytical solution for whirling analysis of axial-loaded Timoshenko rotor is presented and corresponding basic functions are derived. The set of governing equations for whirling analysis of the rotor consists of four coupled partial differential equations; using complex displacements, these equations can be reduced to two coupled partial differential equations. The versatility of the proposed solution is confirmed using published results and the effect of angular velocity of spin, axial load, slenderness and Poisson's ratio on the natural frequencies of the rotor are investigated.

1. Introduction

The Rotor Dynamics is concerned with study of dynamic and stability characteristics of the rotating machineries and plays an important role in the improving safety and performance of the systems. As the rotational velocity of a rotor increases, its level of vibration often passes through critical speeds, commonly excited by unbalance of the rotating structure. If the amplitude of vibration at these critical speeds is excessive, catastrophic failure can occur. Axial loads have significant effect on dynamic characteristics of structures. In the case of rotors, axial force can be generated by several types of gears or thermal effects. Some practical applications of rotor dynamics can be listed as rotating shafts, turbines, aerospace devices, etc. In Euler-Bernoulli beam theory, rotary inertia of the beam element is not considered; therefore, this theory is unable to model gyroscopic effect and cannot distinguish between stationary and rotating beams (Genta, 2007). Hence, to model rotors, it is better to use Timoshenko beam theory. This theory can be used for investigating frequency response of both large and nano scale structures (Torabi et al., 2013a; Samaei, 2015) at Using finite element method, Nelson (1980) studied the vibration analysis of the Timoshenko rotor with internal damping under axial load and Edney et al. (1990) proposed dynamic analysis of the tapered Timoshenko rotor. They considered

* Corresponding author.
E-mail addresses: kvntrb@kashanu.ac.ir (K. Torabi)

doi: 10.5267/j.esm.2015.11.001

viscous and hysteretic material damping, mass eccentricity and axial torque. Grybos (1991) investigated the effect of shear deformation and rotary inertia of a rotor on its critical speeds. An exact solution for vibration analysis of the Timoshenko rotor with general boundary conditions proposed by Zu and Han (1992). Choi et al. (1992) presented the consistent derivation of a set of governing differential equations describing the vibration in two orthogonal planes and the torsional vibration of a straight rotor with dissimilar lateral principal moments of inertia, subjected to a constant compressive axial load. Jun and Kim (1999) studied free bending vibration of a rotating shaft under a constant torsional torque. They modeled rotor as a Timoshenko beam and gyroscopic effect and at each part of the shaft a constant torque were considered. Effect of shaft rotation on its natural frequency was investigated by Behzad and Bastami (2004). They studied natural frequencies by considering the gyroscopic effect, axial force originated from centrifugal force and Poisson's effect. Banerjee and Su (2006) derived dynamic stiffness formulation of a composite spinning beams and studied the vibration analysis of composite rotors. The most advantage of their work was the inclusion of the bending-torsion coupling effect that arises from the ply orientation and stacking sequence in laminated fibrous composites. Hosseini and Khadem (2009) studied vibrations of an in-extensional simply supported rotating shaft with nonlinear curvature and inertia. In their research rotary inertia and gyroscopic effects were considered, but shear deformation was neglected. For large amplitude vibrations, which lead to nonlinearities in curvature and inertia, Hosseini et al. (2014) used method of multiple scales and investigated free vibration and primary resonances of an in-extensional spinning beam with six general boundary conditions. Using differential quadrature element method, Afshari et al. (2014) presented a numerical solution for whirling analysis of multi-step multi-span Timoshenko rotors. In their work no limitation was considered in number of steps and bearings.

In this paper, an exact solution for whirling analysis of Timoshenko rotor subjected to axial load is presented. Corresponding basic functions are derived and effect of angular velocity of spin, axial load, slenderness and Poisson's ratio on the forward and backward frequencies of the rotor are investigated. Regardless using basic functions, the characteristic equation of the rotor depends on a determinant solution of order 4; but the presented basic functions reduce order of final characteristic determinant to 2. Moreover, the most advantage of the basic functions will appear in analysis of rotors with local discontinuities where order of final characteristic determinant be kept as 2 for rotors with any number of local discontinuities; e.g. concentrated masses, cracks, interior spans or steps. These problems can be considered as interesting topics for future studies.

2. Solution procedure

As depicted in Fig. 1, a uniform rotor of length L, diameter d, rotating at constant angular velocity Ω, and subjected to uniform axial load P is considered. Using Timoshenko beam theory, the set of governing equations of free vibration can be stated as (Genta, 2007)

$$kGA\left(\frac{\partial^2 u_x}{\partial z^2}-\frac{\partial \varphi_y}{\partial z}\right)+P\frac{\partial^2 u_x}{\partial z^2}-\rho A\frac{\partial^2 u_x}{\partial t^2}=0, \tag{1-a}$$

$$kGA\left(\frac{\partial^2 u_y}{\partial z^2}+\frac{\partial \varphi_x}{\partial z}\right)+P\frac{\partial^2 u_y}{\partial z^2}-\rho A\frac{\partial^2 u_y}{\partial t^2}=0, \tag{1-b}$$

$$EI_x\frac{\partial^2 \varphi_x}{\partial z^2}-kGA\left(\frac{\partial u_y}{\partial z}+\varphi_x\right)-\rho I_p\Omega\frac{\partial \varphi_y}{\partial t}-\rho I_x\frac{\partial^2 \varphi_x}{\partial t^2}=0, \tag{1-c}$$

$$EI_y\frac{\partial^2 \varphi_y}{\partial z^2}+kGA\left(\frac{\partial u_x}{\partial z}-\varphi_y\right)+\rho I_p\Omega\frac{\partial \varphi_x}{\partial t}-\rho I_y\frac{\partial^2 \varphi_y}{\partial t^2}=0, \tag{1-d}$$

where $u_x(z,t)$, $u_y(z,t)$, $\varphi_x(z,t)$ and $\varphi_y(z,t)$ are components of displacement and rotation in x and y directions, respectively; ρ, E and G are mass density, modulus of elasticity and shear modulus, respectively; Also, A, I_x, I_y and I_p are cross-sectional area, moment of inertia about the x and y axis and

polar moment of inertia, respectively; and k is shear correction factor which depends on the shape of the section and Poisson's ratio of material (Hutchinson, 2001).

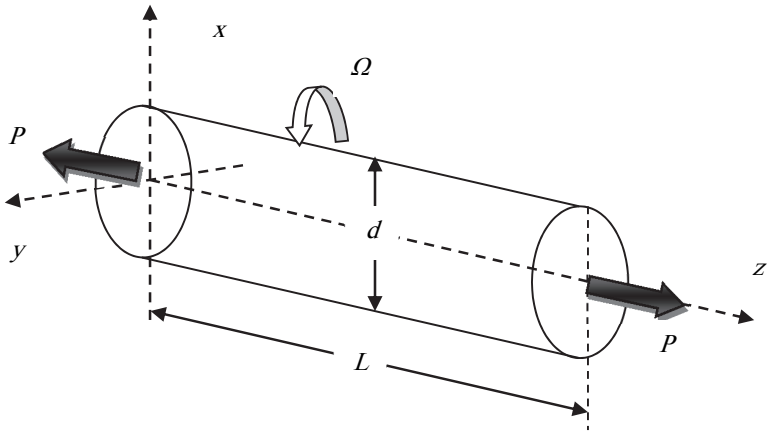

Fig. 1. Axial-loaded Timoshenko rotor

According to Timoshenko beam theory, components of bending moment (M) and shear force (F) in x and y directions are presented as (Genta, 2007)

$$M_x = EI\frac{\partial \varphi_x}{\partial z} \quad M_y = EI\frac{\partial \varphi_y}{\partial z} \quad F_x = kGA\left(\frac{\partial u_x}{\partial z} - \varphi_y\right) + P\frac{\partial u_x}{\partial z} \quad F_y = kGA\left(\frac{\partial u_y}{\partial z} + \varphi_x\right) + P\frac{\partial u_y}{\partial z}. \tag{2}$$

Using following relation for a circular section:

$$I_p = 2I_x = 2I_y = 2I\ . \tag{3}$$

Eqs. (1-c) and (1-d) can be written as

$$EI\frac{\partial^2 \varphi_x}{\partial z^2} - kGA\left(\frac{\partial u_y}{\partial z} + \varphi_x\right) - 2\rho I\,\Omega\frac{\partial \varphi_y}{\partial t} - \rho I\frac{\partial^2 \varphi_x}{\partial t^2} = 0. \tag{4-a}$$

$$EI\frac{\partial^2 \varphi_y}{\partial z^2} + kGA\left(\frac{\partial u_x}{\partial z} - \varphi_y\right) + 2\rho I\,\Omega\frac{\partial \varphi_x}{\partial t} - \rho I\frac{\partial^2 \varphi_y}{\partial t^2} = 0. \tag{4-b}$$

By introducing following complex variables (i^2=-1):

$$u = u_x + iu_y \quad \varphi = \varphi_x + i\,\varphi_y \tag{5}$$

Eq. (1-a), Eq. (1-b), Eq. (4-a) and Eq. (4-b) reduce to

$$kGA\left(\frac{\partial^2 u}{\partial z^2} + i\frac{\partial \varphi}{\partial z}\right) + P\frac{\partial^2 u}{\partial z^2} - \rho A\frac{\partial^2 u}{\partial t^2} = 0, \tag{6-a}$$

$$EI\frac{\partial^2 \varphi}{\partial z^2} + kGA\left(i\frac{\partial u}{\partial z} - \varphi\right) + 2i\,\rho I\,\Omega\frac{\partial \varphi}{\partial t} - \rho I\frac{\partial^2 \varphi}{\partial t^2} = 0, \tag{6-b}$$

and complex forms of bending moment and shear force (Eq. (2)) can be written as

$$m = M_x + iM_y = EI\frac{\partial \varphi}{\partial z} \quad f = F_x + iF_y = kGA\left(\frac{\partial u}{\partial z} + i\,\varphi\right) + P\frac{\partial u}{\partial z}. \tag{7}$$

Uncoupling u and φ in Eq. (6-a) and Eq. (6-b) yields the following relations:

$$\frac{\partial \varphi}{\partial z} = i\left[\left(1 + \frac{P}{kGA}\right)\frac{\partial^2 u}{\partial z^2} - \frac{\rho}{kG}\frac{\partial^2 u}{\partial t^2}\right]. \tag{8-a}$$

$$EI\left(1+\frac{P}{kGA}\right)\frac{\partial^4 u}{\partial z^4}-\rho I\left(1+\frac{E}{kG}+\frac{P}{kGA}\right)\frac{\partial^4 u}{\partial z^2\partial t^2}+2i\,\rho I\Omega\left(1+\frac{P}{kGA}\right)\frac{\partial^3 u}{\partial z^2\partial t}$$
$$-P\frac{\partial^2 u}{\partial z^2}+\frac{\rho^2 I}{kG}\frac{\partial^4 u}{\partial t^4}-2i\,\frac{\rho^2 I\Omega}{kG}\frac{\partial^3 u}{\partial t^3}+\rho A\frac{\partial^2 u}{\partial t^2}=0 \tag{8-b}$$

Introducing ω as the circular natural frequency of whirling, ζ=z/L as the dimensionless spatial variable and also using the method of separation of variables as

$$u(\zeta,t)=Lv(\zeta)e^{i\omega t}\quad \varphi(\zeta,t)=\psi(\zeta)e^{i\omega t} \tag{9}$$

Eq. (8-a) and Eq. (8-b) can be written in the following dimensionless form:

$$\psi'=i\left[s^2\lambda^2 v+\left(1+P^*\right)v''\right], \tag{10-a}$$

$$v^{(4)}+2d_1 v''+d_2 v=0, \tag{10-b}$$

where the prime indicates the derivative with respect to the dimensionless spatial variable (ζ) and the following dimensionless parameters are defined:

$$r=\frac{d}{4L}\quad s^2=\frac{2(1+\upsilon)}{k}r^2\quad P^*=\frac{P}{kGA}\quad \gamma^2=\frac{\rho AL^4\Omega^2}{EI}$$
$$\lambda^2=\frac{\rho AL^4\omega^2}{EI}\quad d_1=\frac{s^4\lambda^2-P^*}{2s^2\left(1+P^*\right)}+\frac{r^2\lambda(\lambda-2\gamma)}{2}\quad d_2=\lambda^2\frac{s^2r^2\lambda(\lambda-2\gamma)-1}{1+P^*} \tag{11}$$

In the whirling analysis of rotors, two kind of frequencies can be considered. When whirling and spin of the rotor are in the same direction (Ωω>0), forward whirling occurs and when they are in opposite directions (Ωω<0), backward one occurs. Solution of Eqs. (10-a) and (10-b) depends on the sign of d_2 which differs at low and high modes. In practice, lower frequencies are more important than higher ones and d_2 is a negative parameter at these modes, thus following solution can be found (Torabi et al., 2013b):

$$v(\zeta)=v_0\left[A\cosh(\beta_1\zeta)+B\sinh(\beta_1\zeta)+C\cos(\beta_2\zeta)+D\sin(\beta_2\zeta)\right]$$
$$\psi(\zeta)=iv_0\left[Am_1\sinh(\beta_1\zeta)+Bm_1\cosh(\beta_1\zeta)+Cm_2\sin(\beta_2\zeta)-Dm_2\cos(\beta_2\zeta)\right] \tag{12}$$

in which v_0 is a complex coefficient and

$$m_1=\frac{\beta_1^2+s^2\lambda^2}{\beta_1}\quad m_2=\frac{-\beta_2^2+s^2\lambda^2}{\beta_2}\quad \beta_1=\sqrt{-d_1+\sqrt{d_1^2-d_2}}\quad \beta_2=\sqrt{d_1+\sqrt{d_1^2-d_2}}\,. \tag{13}$$

Also, bending moment and shear force can be written as

$$m(\zeta,t)=\frac{EI}{L}M(\zeta)e^{i\omega t}\quad f(\zeta,t)=kGAF(\zeta)e^{i\omega t}, \tag{14}$$

in which

$$M(\zeta)=\psi'\quad F(\zeta)=\left(1+P^*\right)v'+i\psi \tag{15}$$

3. Basic functions

In order to derive basic functions, first, consider following definitions for trigonometric and hyperbolic functions:

$$S_1=\cosh(\beta_1\zeta)\quad S_2=\sinh(\beta_1\zeta)\quad S_3=\cos(\beta_2\zeta)\quad S_4=\sin(\beta_2\zeta)$$
$$T_1=im_1\sinh(\beta_1\zeta)\quad T_2=im_1\cosh(\beta_1\zeta)\quad T_3=im_2\sin(\beta_2\zeta)\quad T_4=-im_2\cos(\beta_2\zeta) \tag{16}$$

which are defined according to Eq. (12). Geometrical basic functions will be defined to satisfy following constraints:

$$\begin{aligned}
&\overline{S}_1(0)=1 \quad \overline{S}'_1(0)=0 \quad \overline{T}_1(0)=0 \quad \overline{T}'_1(0)=0\\
&\overline{S}_2(0)=0 \quad \overline{S}'_2(0)=1 \quad \overline{T}_2(0)=0 \quad \overline{T}'_2(0)=0\\
&\overline{S}_3(0)=0 \quad \overline{S}'_3(0)=0 \quad \overline{T}_3(0)=1 \quad \overline{T}'_3(0)=0\\
&\overline{S}_4(0)=0 \quad \overline{S}'_4(0)=0 \quad \overline{T}_4(0)=0 \quad \overline{T}'_4(0)=1
\end{aligned} \tag{17}$$

Now, displacement and rotation, can be stated in terms of their values at the left side of the rotor (ζ=0) and the geometrical basic functions as:

$$\begin{aligned}
v(\zeta)&=v(0)\overline{S}_1(\zeta)+v'(0)\overline{S}_2(\zeta)+\psi(0)\overline{S}_3(\zeta)+\psi'(0)\overline{S}_4(\zeta)\\
\psi(\zeta)&=v(0)\overline{T}_1(\zeta)+v'(0)\overline{T}_2(\zeta)+\psi(0)\overline{T}_3(\zeta)+\psi'(0)\overline{T}_4(\zeta)
\end{aligned} \tag{18}$$

In order to obtain geometrical basic functions in terms of S_1-T_4, following relation are considered:

$$\overline{S}_i=\sum_{j=1}^{4}A_{ij}S_j \quad \overline{T}_i=\sum_{j=1}^{4}A_{ij}T_j \tag{19}$$

Substituting Eq. (16) and Eq. (17) into the Eq. (19), following relation will be obtained:

$$\begin{bmatrix}
\overline{S}_1(0) & \overline{S}'_1(0) & \overline{T}_1(0) & \overline{T}'_1(0)\\
\overline{S}_2(0) & \overline{S}'_2(0) & \overline{T}_2(0) & \overline{T}'_2(0)\\
\overline{S}_3(0) & \overline{S}'_3(0) & \overline{T}_3(0) & \overline{T}'_3(0)\\
\overline{S}_4(0) & \overline{S}'_4(0) & \overline{T}_4(0) & \overline{T}'_4(0)
\end{bmatrix}=[A]\begin{bmatrix}
S_1(0) & S'_1(0) & T_1(0) & T'_1(0)\\
S_2(0) & S'_2(0) & T_2(0) & T'_2(0)\\
S_3(0) & S'_3(0) & T_3(0) & T'_3(0)\\
S_4(0) & S'_4(0) & T_4(0) & T'_4(0)
\end{bmatrix} \tag{20}$$

Using Eq. (20), the coefficients of Eq. (19) can be obtained as

$$[A]=\begin{bmatrix}
\dfrac{-m_2\beta_2}{m_1\beta_1-m_2\beta_2} & 0 & \dfrac{m_1\beta_1}{m_1\beta_1-m_2\beta_2} & 0\\
0 & \dfrac{m_2}{m_2\beta_1+m_1\beta_2} & 0 & \dfrac{m_1}{m_2\beta_1+m_1\beta_2}\\
0 & -\dfrac{i\beta_2}{m_2\beta_1+m_1\beta_2} & 0 & \dfrac{i\beta_1}{m_2\beta_1+m_1\beta_2}\\
\dfrac{-i}{m_1\beta_1-m_2\beta_2} & 0 & \dfrac{i}{m_1\beta_1-m_2\beta_2} & 0
\end{bmatrix} \tag{21}$$

which leads to

$$\begin{cases}
\overline{S}_1(\zeta)=\dfrac{1}{m_1\beta_1-m_2\beta_2}\left[-m_2\beta_2\cosh(\beta_1\zeta)+m_1\beta_1\cos(\beta_2\zeta)\right]\\
\overline{S}_2(\zeta)=\dfrac{1}{m_2\beta_1+m_1\beta_2}\left[m_2\sinh(\beta_1\zeta)+m_1\sin(\beta_2\zeta)\right]\\
\overline{S}_3(\zeta)=\dfrac{i}{m_2\beta_1+m_1\beta_2}\left[-\beta_2\sinh(\beta_1\zeta)+\beta_1\sin(\beta_2\zeta)\right]\\
\overline{S}_4(\zeta)=\dfrac{i}{m_1\beta_1-m_2\beta_2}\left[-\cosh(\beta_1\zeta)+\cos(\beta_2\zeta)\right]
\end{cases}$$

$$\begin{cases}
\overline{T}_1(\zeta)=\dfrac{im_1m_2}{m_1\beta_1-m_2\beta_2}\left[-\beta_2\sinh(\beta_1\zeta)+\beta_1\sin(\beta_2\zeta)\right]\\
\overline{T}_2(\zeta)=\dfrac{im_1m_2}{m_2\beta_1+m_1\beta_2}\left[\cosh(\beta_1\zeta)-\cos(\beta_2\zeta)\right]\\
\overline{T}_3(\zeta)=\dfrac{1}{m_2\beta_1+m_1\beta_2}\left[m_1\beta_2\cosh(\beta_1\zeta)+m_2\beta_1\cos(\beta_2\zeta)\right]\\
\overline{T}_4(\zeta)=\dfrac{1}{m_1\beta_1-m_2\beta_2}\left[m_1\sinh(\beta_1\zeta)-m_2\sin(\beta_2\zeta)\right]
\end{cases} \tag{22}$$

Eight functions, presented in Eq. (22) are known as geometrical basic functions which are useful just for clamped boundary conditions; for convenience in implementation of all boundary conditions, it is better to use physical basic functions instead of geometrical ones. Using Eq. (15), one can write

$$\begin{Bmatrix} v(0) \\ \psi(0) \\ M(0) \\ F(0) \end{Bmatrix} = \begin{bmatrix} 1 & 0 & 0 & 0 \\ 0 & 0 & 1 & 0 \\ 0 & 0 & 0 & 1 \\ 0 & 1 & i & 0 \end{bmatrix} \begin{Bmatrix} v(0) \\ v'(0) \\ \psi(0) \\ \psi'(0) \end{Bmatrix} \tag{23}$$

which leads to

$$\begin{Bmatrix} v(0) \\ v'(0) \\ \psi(0) \\ \psi'(0) \end{Bmatrix} = \begin{bmatrix} 1 & 0 & 0 & 0 \\ 0 & -i & 0 & 1 \\ 0 & 1 & 0 & 0 \\ 0 & 0 & 1 & 0 \end{bmatrix} \begin{Bmatrix} v(0) \\ \psi(0) \\ M(0) \\ V(0) \end{Bmatrix}. \tag{24}$$

substitution of Eq. (24) into the Eq. (18) leads to the following relations:

$$\begin{aligned} v(\zeta) &= v(0) f_1(\zeta) + \Psi(0) f_2(\zeta) + M(0) f_3(\zeta) + F(0) f_4(\zeta), \\ \psi(\zeta) &= v(0) g_1(\zeta) + \Psi(0) g_2(\zeta) + M(0) g_3(\zeta) + F(0) g_4(\zeta), \end{aligned} \tag{25}$$

where following natural basic functions are defined:

$$\begin{aligned} &f_1 = \overline{S}_1 \quad f_2 = \overline{S}_3(\zeta) - i\overline{S}_2(\zeta) \quad f_3 = \overline{S}_4 \quad f_4 = \overline{S}_2, \\ &g_1 = \overline{T}_1 \quad g_2 = \overline{T}_3(\zeta) - i\overline{T}_2(\zeta) \quad g_3 = \overline{T}_4 \quad g_4 = \overline{T}_2. \end{aligned} \tag{26}$$

Using Eq. (22) and Eq. (26), one can write:

$$\begin{cases} f_1(\zeta) = \dfrac{-1}{m_1\beta_1 - m_2\beta_2}\left[m_2\beta_2\cosh(\beta_1\zeta) - m_1\beta_1\cos(\beta_2\zeta)\right] \\ f_2(\zeta) = -i\dfrac{1}{m_2\beta_1 + m_1\beta_2}\left[(m_2+\beta_2)\sinh(\beta_1\zeta) + (m_1-\beta_1)\sin(\beta_2\zeta)\right] \\ f_3(\zeta) = -i\dfrac{1}{m_1\beta_1 - m_2\beta_2}\left[\cosh(\beta_1\zeta) - \cos(\beta_2\zeta)\right] \\ f_4(\zeta) = \dfrac{1}{m_2\beta_1 + m_1\beta_2}\left[m_2\sinh(\beta_1\zeta) + m_1\sin(\beta_2\zeta)\right] \end{cases}$$

$$\begin{cases} g_1(\zeta) = -i\dfrac{m_1 m_2}{m_1\beta_1 - m_2\beta_2}\left[\beta_2\sinh(\beta_1\zeta) - \beta_1\sin(\beta_2\zeta)\right] \\ g_2(\zeta) = \dfrac{1}{m_2\beta_1 + m_1\beta_2}\left[m_1(m_2+\beta_2)\cosh(\beta_1\zeta) - m_2(m_1-\beta_1)\cos(\beta_2\zeta)\right] \\ g_3(\zeta) = \dfrac{1}{m_1\beta_1 - m_2\beta_2}\left[m_1\sinh(\beta_1\zeta) - m_2\sin(\beta_2\zeta)\right] \\ g_4(\zeta) = i\dfrac{m_1 m_2}{m_2\beta_1 + m_1\beta_2}\left[\cosh(\beta_1\zeta) - \cos(\beta_2\zeta)\right] \end{cases} \tag{27}$$

4. Implementation of boundary conditions

Three standard condition for each end of the rotor is considered as simple (pinned), clamped and free. Mathematical model of these conditions are listed in Table 1.

Table 1. Mathematical model of boundary conditions

Boundary conditions	Simple (S)	Clamped (C)	Free (F)
Mathematical model	$v=0 \quad M=0$	$v=0 \quad \psi=0$	$M=0 \quad F=0$

For a simply supported rotor, boundary conditions at ζ=0, are v(0)=0 and M(0)=0 which lead to

$$\begin{aligned} v(\zeta) &= \psi(0) f_2(\zeta) + F(0) f_4(\zeta), \\ \psi(\zeta) &= \psi(0) g_2(\zeta) + F(0) g_4(\zeta). \end{aligned} \tag{28}$$

Substituting Eq. (28) into the boundary conditions at ζ=1 which are v(1)=0 and M(1)=0 leads to

$$\begin{bmatrix} f_2(1) & f_4(1) \\ g_2'(1) & g_4'(1) \end{bmatrix} \begin{Bmatrix} \psi(0) \\ F(0) \end{Bmatrix} = \begin{Bmatrix} 0 \\ 0 \end{Bmatrix}. \tag{29}$$

For a simple-clamped rotor, conditions at ζ=0 are same with the simply supported rotor, substituting Eq. (28) into the boundary conditions at ζ=1 which are v(1)=0 and ψ(1)=0 leads to

$$\begin{bmatrix} f_2(1) & f_4(1) \\ g_2(1) & g_4(1) \end{bmatrix} \begin{Bmatrix} \psi(0) \\ F(0) \end{Bmatrix} = \begin{Bmatrix} 0 \\ 0 \end{Bmatrix}. \tag{30}$$

In a similar manner, for a clamped-clamped rotor, boundary conditions at ζ=0 are v(0)=0 and ψ(0)=0 which lead to

$$\begin{aligned} v(\zeta) &= M(0) f_3(\zeta) + F(0) f_4(\zeta), \\ \psi(\zeta) &= M(0) g_3(\zeta) + F(0) g_4(\zeta). \end{aligned} \tag{31}$$

substituting Eq. (31) into the boundary conditions at ζ=1 which are v(1)=0 and ψ(1)=0 leads to

$$\begin{bmatrix} f_3(1) & f_4(1) \\ g_3(1) & g_4(1) \end{bmatrix} \begin{Bmatrix} M(0) \\ F(0) \end{Bmatrix} = \begin{Bmatrix} 0 \\ 0 \end{Bmatrix}. \tag{32}$$

For a clamped-free rotor, conditions at ζ=0 are same with the clamped-clamped rotor, substituting Eq. (31) into the boundary conditions at ζ=1 which are M(1)=0 and F(1)=0 leads to

$$\begin{bmatrix} g_3'(1) & g_4'(1) \\ \left(1+P^*\right) f_3'(1) + i g_3(1) & \left(1+P^*\right) f_4'(1) + i g_4(1) \end{bmatrix} \begin{Bmatrix} M(0) \\ F(0) \end{Bmatrix} = \begin{Bmatrix} 0 \\ 0 \end{Bmatrix}. \tag{33}$$

Using Eq. (29), Eq. (30), Eq. (32) or Eq. (33) dimensionless natural frequencies can be obtained and also corresponding mode shapes can be derived in an exact closed form for all standard boundary conditions.

5. Results and discussion

Here the numerical results are presented for the developed analytical solution in the previous sections. Consider a simply supported uniform Timoshenko rotor with r=0.03, s=0.05, γ=5, P^*=0. In Table 2 value of the first four forward and backward frequencies are presented and are compared with whose which can be easily derived using sinusoidal modes as (Genta, 2007)

$$\lambda^4 - 2i\gamma\lambda^3 + \frac{1+\left(r^2+s^2\right)n^2\pi^2}{r^2 s^2}\lambda^2 - 2i\gamma\frac{n^2\pi^2}{s^2}\lambda + \frac{n^4\pi^4}{r^2 s^2} = 0. \tag{34}$$

Table 2. Value of the first four frequencies of a simply supported rotor

	Forward whirling				Backward whirling			
	λ_1	λ_2	λ_3	λ_4	λ_1	λ_2	λ_3	λ_4
Present	9.75293	37.28796	78.62959	129.5721	9.665039	36.94528	77.89286	128.3437
Genta, 2007	9.751104	37.2636	78.5207	129.316	9.667179	36.9761	78.0016	128.600

As Table 2 shows, results with high accuracies can be obtained. A rotor with r=0.03, s=0.05 and P^*=0.1 is considered. For first two modes, Campbell diagram is depicted in Figs. 2.a-2.d for all standard

boundary conditions. As shown in these figures, for a stationary rotor, value of the forward and backward frequencies have the same values; but because of the gyroscopic effect, as value of the velocity of spin grows, forward frequencies increase and backward ones decrease. In other words value of the each backward frequency is less than corresponding value of the forward one. This figures also show the line of synchronous whirling; intersection of this line with the Campbell diagram determines the critical speeds which should be avoided.

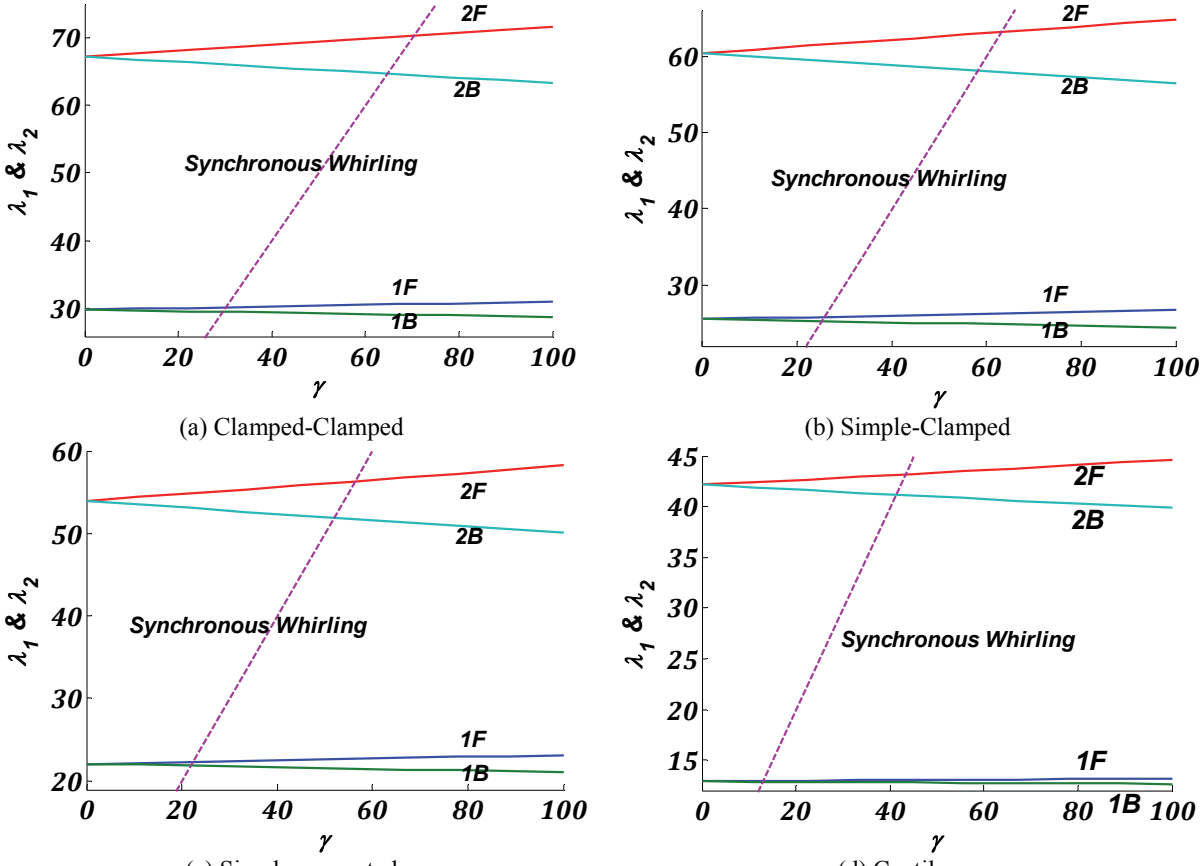

(a) Clamped-Clamped (b) Simple-Clamped

(c) Simply supported (d) Cantilever

Fig. 2. Campbell diagram for first two modes of a rotor in four cases of boundary conditions

Also for γ=100, corresponding mode shapes are depicted in Figs (3.a-3.d). Difference between forward and backward modes can be easily seen in these figures.

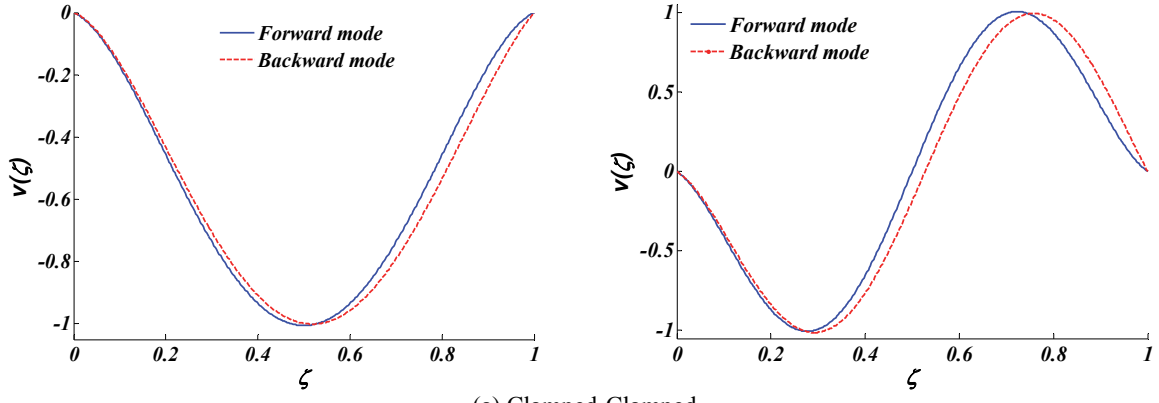

(a) Clamped-Clamped

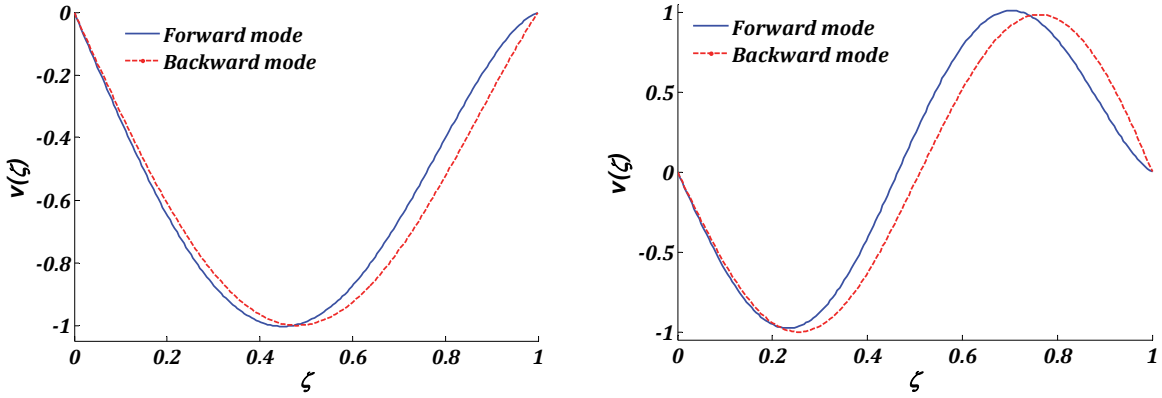

(b) Simple-Clamped

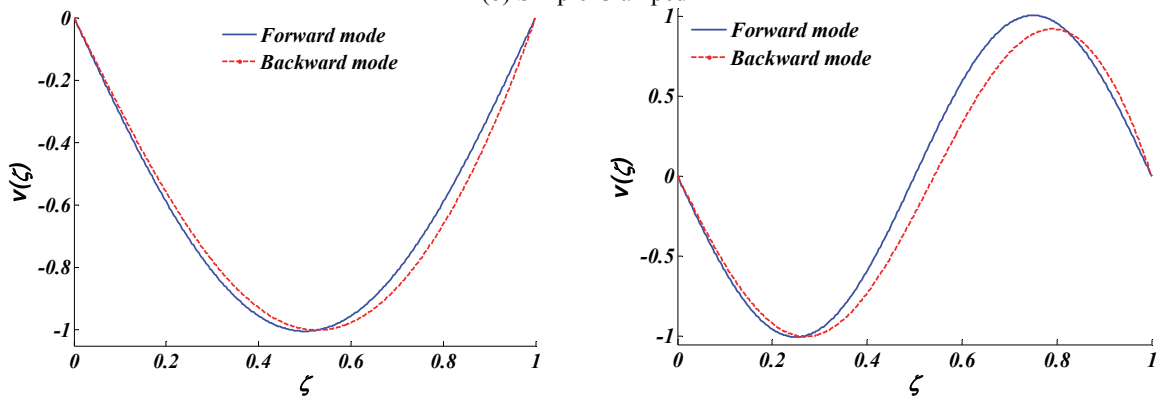

(c) Simply Supported

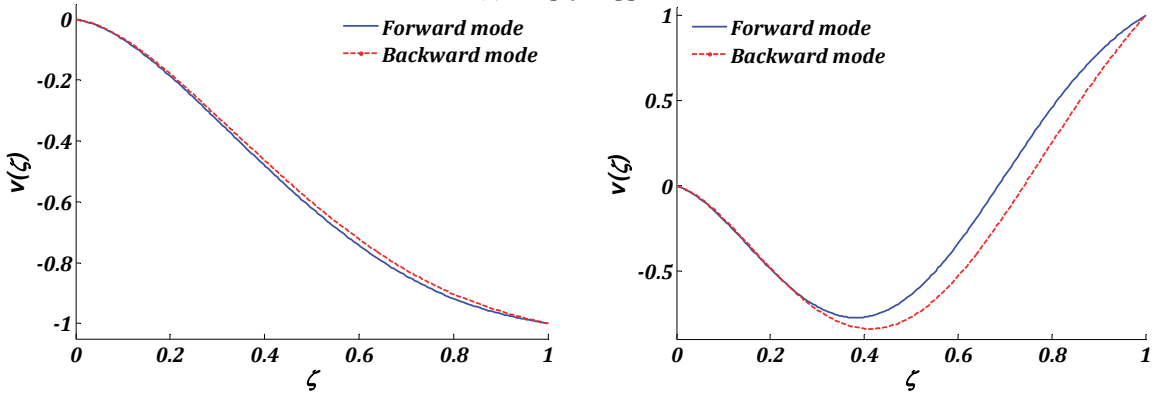

(d) Cantilever

Fig. 3. First two forward and backward mode shapes of rotor for γ=100

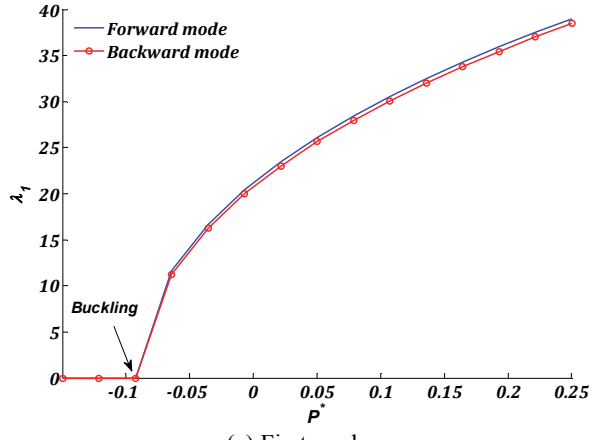

(a) First mode

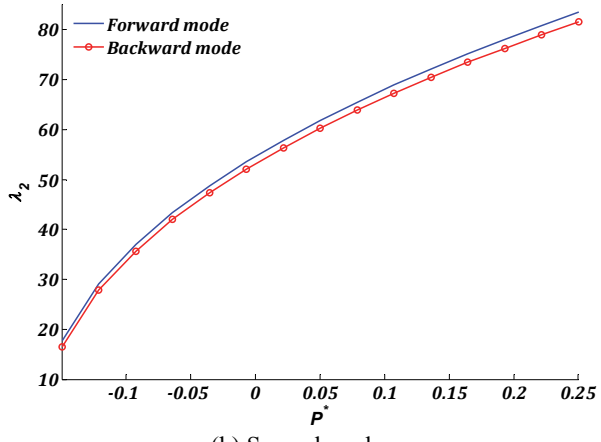

(b) Second mode

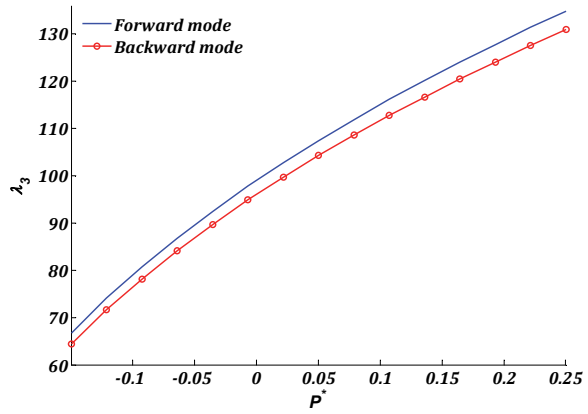

(c) Third mode

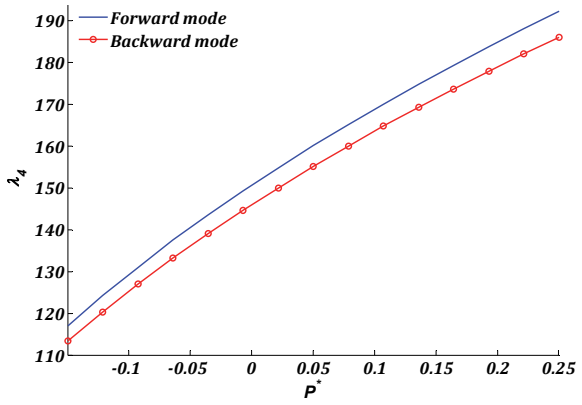

(d) Fourth mode

Fig. 4. Effect of axial load on the first four forward and backward frequencies of a clamped-clamped rotor

Now, consider a clamped-clamped rotor with r=0.03, s=0.05 and γ=20. Figs. (4.a- 4.d) show value of the first four forward and backward frequencies versus value of the axial load. As is anticipated, tension load leads to increase in the all frequencies whereas compressive one decreases all frequencies. It should be noticed that because of applied compressive load, some lower frequencies reach to zero and buckling and instability of the rotor happen. It is obvious that buckling will happen at the first backward mode earlier than other modes.

In order to investigate the effect of slenderness and Poisson's ratio on forward and backward frequencies, it is better to use the following new dimensionless frequency:

$$\Lambda^2 = \frac{\rho L^2 \omega^2}{E} = r^2 \lambda^2 \tag{35}$$

A simply supported rotor with γ=50 and P^*=0.1 is considered. For various values of Poisson's ratio, variation of the first four forward and backward frequencies is illustrated in Figs. 5.a-5.d versus slenderness ratio. As shown in these figures, increasing in diameter of the rotor increases value of the whole forward and backward frequencies. It should be noted that as value of the diameter increases, both stiffness (K) and mass (M) of the rotor increase; but value of the increase for stiffness is more than increase in mass ($K \propto d^4$, $M \propto d^2$). This figures also show that as value of the Poisson's ratio increases, a gentle decrease in all forward and backward frequencies can be seen. It can be explained by increasing in flexibility of material.

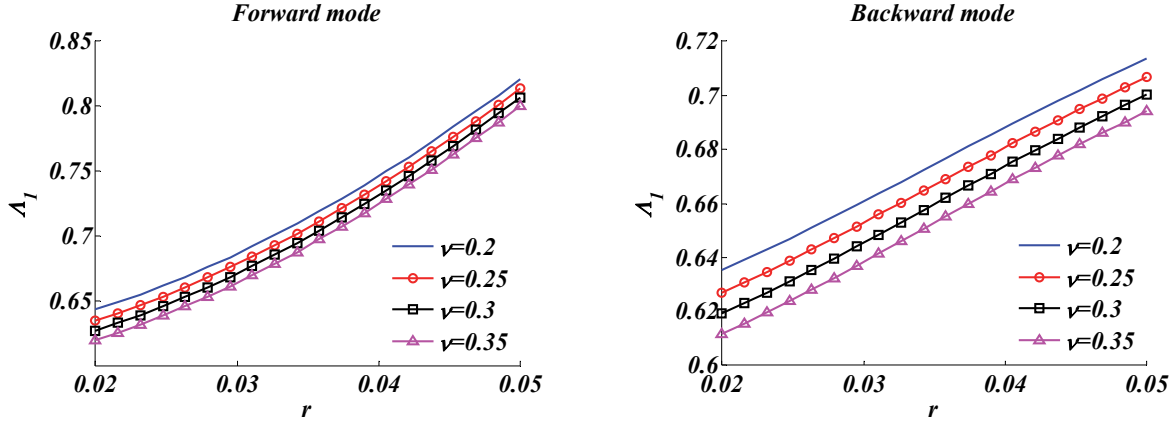

(a) First mode

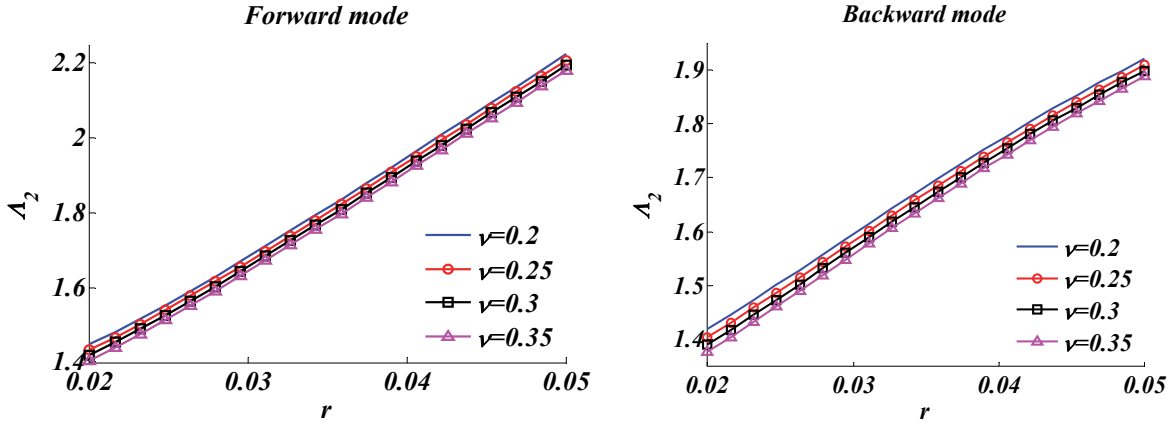

(b) Second mode

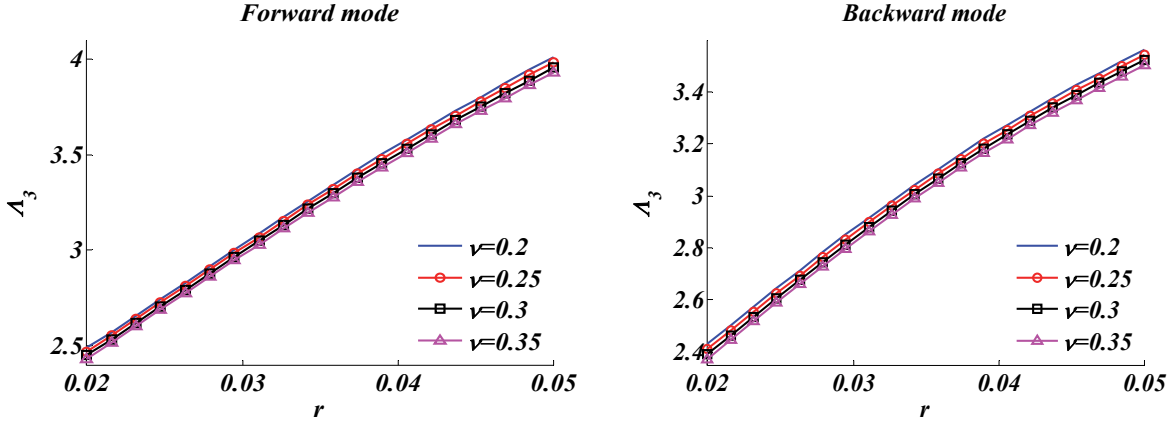

(c) Third mode

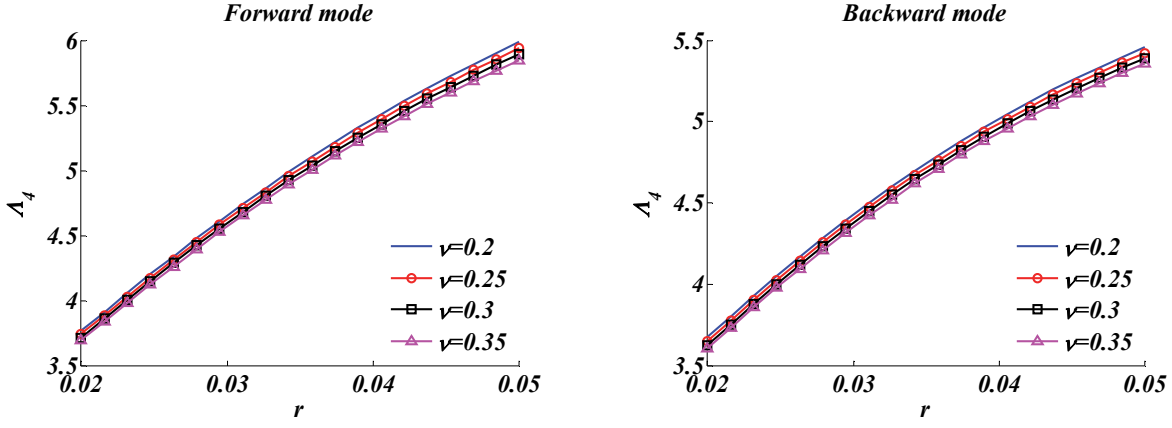

(d) Fourth mode

Fig. 5. Variation of the first four forward and backward frequencies versus slenderness ratio and various values of Poisson's ratio

It is worth mentioning that for Figs. 5.a-5.d, shear correction factor is calculated using following relation (Hutchinson, 2001):

$$k = \frac{6(1+\upsilon)^2}{7+12\upsilon+4\upsilon^2} \tag{36}$$

6. Conclusions

Basic functions were derived to present an exact solution for whirling analysis of Timoshenko rotor subjected to constant axial load. Using presented analytical solution, effect of angular velocity of spin, axial load, slenderness and Poisson's ratio on the forward and backward frequencies were investigated. Numerical results showed that for a stationary beam, value of the forward and backward frequencies have the same values; but as value of the velocity of spin grows, forward frequencies increase and backward ones decrease. Numerical examples also confirms that tension axial load leads to increase in the all frequencies whereas compressive one decreases all frequencies. It also was concluded that increasing in diameter of the rotor increases value of the all frequencies and increase in value of the Poisson's ratio decrease all frequencies.

References

Afshari, H., Irani M. & Torabi K. (2014). Free whirling analysis of multi-step Timoshenko rotor with multiple bearing using DQEM. *Modares Mechanical Engineering*, *14*, 109-120 (In Persian).

Banerjee, J. R., & Su, H. (2006). Dynamic stiffness formulation and free vibration analysis of a spinning composite beam. *Computers & Structures*, *84*(19), 1208-1214.

Behzad, M., & Bastami, A. R. (2004). Effect of centrifugal force on natural frequency of lateral vibration of rotating shafts. *Journal of Sound and Vibration*, *274*(3), 985-995.

Choi, S. H., Pierre, C., & Ulsoy, A. G. (1992). Consistent modeling of rotating Timoshenko shafts subject to axial loads. *Journal of Vibration and Acoustics*, *114*(2), 249-259.

Edney, S. L., Fox, C. H. J., & Williams, E. J. (1990). Tapered Timoshenko finite elements for rotor dynamics analysis. *Journal of sound and vibration*, *137*(3), 463-481.

Genta, G. (2007). *Dynamics of rotating systems*. Springer Science & Business Media.

Grybos, R. (1991). The effect of shear and rotary inertia of a rotor at its critical speeds. *Archive of Applied Mechanics*, *61*(2), 104-109.

Hosseini, S. A. A., & Khadem, S. E. (2009). Free vibrations analysis of a rotating shaft with nonlinearities in curvature and inertia. *Mechanism and Machine theory*, *44*(1), 272-288.

Hosseini, S. A. A., Zamanian, M., Shams, S., & Shooshtari, A. (2014). Vibration analysis of geometrically nonlinear spinning beams. *Mechanism and Machine Theory*, *78*, 15-35.

Hutchinson, J. R. (2001). Shear coefficients for Timoshenko beam theory. *Journal of Applied Mechanics*, *68*(1), 87-92.

Jun, O. S., & Kim, J. O. (1999). Free bending vibration of a multi-step rotor. *Journal of Sound and Vibration*, *224*(4), 625-642.

Nelson, H. D. (1980). A finite rotating shaft element using Timoshenko beam theory. *Journal of mechanical design*, *102*(4), 793-803.

Samaei, A. T., Aliha, M. R. M., & Mirsayar, M. M. (2015). Frequency analysis of a graphene sheet embedded in an elastic medium with consideration of small scale. *Materials Physics and Mechanics*, *22*, 125-135.

Torabi, K., Afshari, H., & Heidari-Rarani, M. (2013a). Free vibration analysis of a non-uniform cantilever Timoshenko beam with multiple concentrated masses using DQEM. *Engineering Solid Mechanics*, *1*(1), 9-20.

Torabi, K., Afshari, H., & Najafi, H. (2013b). Vibration Analysis of Multi-Step Bernoulli-Euler and Timoshenko Beams Carrying Concentrated Masses. *Journal of Solid Mechanics*, *5*(4), 336-349.

Zu, J. W. Z., & Han, R. P. (1992). Natural frequencies and normal modes of a spinning Timoshenko beam with general boundary conditions. *Journal of Applied Mechanics*, *59*(2S), S197-S204.